

## Higher harmonics generation in relativistic electron beam with virtual cathode

S. A. Kurkin, A. A. Badarin, A. A. Koronovskii, and A. E. Hramov

Citation: *Physics of Plasmas* (1994-present) **21**, 093105 (2014); doi: 10.1063/1.4895507

View online: <http://dx.doi.org/10.1063/1.4895507>

View Table of Contents: <http://scitation.aip.org/content/aip/journal/pop/21/9?ver=pdfcov>

Published by the [AIP Publishing](#)

---

### Articles you may be interested in

[Microwave radiation power of relativistic electron beam with virtual cathode in the external magnetic field](#)

*Appl. Phys. Lett.* **103**, 043507 (2013); 10.1063/1.4816471

[Plasma-based multistage virtual cathode radiation](#)

*Phys. Plasmas* **18**, 123104 (2011); 10.1063/1.3672059

[High power microwave generation from coaxial virtual cathode oscillator using graphite and velvet cathodes](#)

*J. Appl. Phys.* **107**, 093301 (2010); 10.1063/1.3399650

[Instability of relativistic electron-beam–dielectric system as a mechanism for microwave generation](#)

*J. Appl. Phys.* **102**, 103305 (2007); 10.1063/1.2817642

[Forward current propagation beyond the virtual cathode formed by a high injection current](#)

*Appl. Phys. Lett.* **79**, 913 (2001); 10.1063/1.1391408

---



 Vacuum Solutions from a Single Source

- Turbopumps
- Backing pumps
- Leak detectors
- Measurement and analysis equipment
- Chambers and components

**PFEIFFER**  **VACUUM**

## Higher harmonics generation in relativistic electron beam with virtual cathode

S. A. Kurkin,<sup>a)</sup> A. A. Badarin, A. A. Koronovskii, and A. E. Hramov  
 Saratov State Technical University, Politechnicheskaja 77, Saratov 410028, Russia and Saratov State University, Astrakhanskaja 83, Saratov 410012, Russia

(Received 26 July 2014; accepted 29 August 2014; published online 12 September 2014)

The study of the microwave generation regimes with intense higher harmonics taking place in a high-power vircator consisting of a relativistic electron beam with a virtual cathode has been made. The characteristics of these regimes, in particular, the typical spectra and their variations with the change of the system parameters (beam current, the induction of external magnetic field) as well as physical processes occurring in the system have been analyzed by means of 3D electromagnetic simulation. It has been shown that the system under study demonstrates the tendency to the sufficient growth of the amplitudes of higher harmonics in the spectrum of current oscillations in the VC region with the increase of beam current. The obtained results allow us to consider virtual cathode oscillators as promising high power mmw-to-THz sources. © 2014 AIP Publishing LLC.  
[\[http://dx.doi.org/10.1063/1.4895507\]](http://dx.doi.org/10.1063/1.4895507)

Relativistic beam-plasma systems using virtual cathode (VC) oscillations for an electromagnetic radiation generation are the perspective devices of vacuum and plasma high-power microwave electronics.<sup>1–3</sup> Virtual cathode oscillators (such as vircators, reditrons, virtodes, etc.) are a special class of bremsstrahlung microwave generators, whose operation is based on the formation of a VC in an electron beam with overcritical current.<sup>1,3–5</sup> At the present time such devices are investigated actively and considered as the sources of the impulses of high-power microwave radiation and as setups for ion acceleration and plasma heating.<sup>1,3,6–10</sup> The important and attractive features of vircators are high output microwave radiation power, a simple construction (particularly, vircators can operate without external focusing magnetic field), the possibility of a simple frequency tuning and regime switching (tunability).<sup>3,6,11–14</sup>

The fundamental generation frequency,  $\omega_{VCO}$ , of known vircator modifications in the absence of an external resonant structure is determined by the plasma frequency,  $\omega_p^0$ , of an undisturbed electron beam (undisturbed plasma frequency) as  $\omega_{VCO} = k_0 \omega_p^0$ , where the coefficient of proportionality,  $k_0$ , is in the range  $[0.5, 2]$  and depends on the configuration of a virtual cathode oscillator (VCO) and operating regime.<sup>3,6,15–17</sup> In practical cases  $\omega_{VCO}$  lies usually in the range<sup>1,20</sup> GHz. At the same time, the creation of effective high-power generators in poorly developed sub-THz/THz ranges is an actual problem of the modern plasma physics and high-power microwave electronics.<sup>18</sup> Such devices may be used for the purposes of spectroscopy, tomography and medical imaging, submillimeter astronomy, communication, security, etc.<sup>18–22</sup>

So, the increase of the generation frequency and the advancement of vircators to a sub-THz range on retention of their high output power are important and actual problems for practical purposes now.<sup>2,3,14</sup> A possible direction for the

improvement of vircator characteristics is the development and design of the new modifications of VCOs that use newly discovered effects occurring in the relativistic and ultra-relativistic electron beams with overcritical currents.<sup>10,16,23,24</sup> A promising way to increase the radiation frequency of a vircator system up to sub-THz range is the use of the higher harmonics of the fundamental frequency of VCOs in the strongly nonlinear regime of a VCO operation. Currently, a generation at higher harmonics is widely applied in gyrotrons.<sup>25–28</sup> It is also known that under certain conditions the beam-plasma systems with the intensive beams of charged particles demonstrate the regimes with developed higher harmonics (see, e.g., Ref. 29 devoted to the investigation of a hollow-cathode discharge process and Ref. 30 where the physics of the turbutron, the high-power pulsed millimeter-wave source consisting of an intensely oscillating turbulent relativistic electron plasma created between the emission and virtual cathodes, is reviewed). Our preliminary studies have also shown that the relativistic electron beam (REB) with the overcritical current demonstrates VCOs with the spectrum comprising the higher harmonics of the fundamental frequency,  $\omega_{VCO}$ . So, there is a significant interest in the studies and development of vircator schemes operating at the higher harmonics of the fundamental frequency of virtual cathode oscillations. It allows to advance these devices to a submillimeter wavelength range on retention of a typical high output power.

Analyzing relativistic vircators, it is necessary to take into account effects being insignificant for the weakly relativistic systems, in particular, the influence of the self-magnetic fields of a REB.<sup>10,24</sup> For that reason, the 3D fully electromagnetic self-consistent CST Particle Studio package is used in our work for the accurate numerical investigations of generation processes in the relativistic vircator model. In this paper, we report the results of the 3D numerical study of higher harmonics generation processes in the relativistic vircator model with the annular REB in the presence of external uniform axial magnetic field.

<sup>a)</sup>Electronic mail: KurkinSA@gmail.com.

The system under study consists of the perfect electric conducting finite-length cylindrical waveguide region (the electron beam drift chamber) of the length  $L$ , the radius  $R$ , with a grid electrode on the left side and a coaxial waveguide port on the right side. An axially-symmetrical monoenergetic annular relativistic electron beam with the current  $I_0$ , the initial electron energy  $W_e$  (850 keV in this work), the external radius  $R_b$  and the thickness  $d$  is injected through the left (entrance) electrode. Electrons can leave the waveguide region by reaching the side wall or the right (collector) end of the drift chamber. In the present paper, the values of the geometric parameters were chosen as:  $L = 45$  mm,  $R = 10$  mm,  $R_b = 5$  mm,  $d = 1.5$  mm. The resonant properties of the system do not appear practically because it is superdimensional waveguide in respect of a wavelength corresponding to a vircator fundamental frequency. The external uniform magnetic field with induction  $B_z = B_0 \in (0, 2)$  T is applied along the longitudinal axis of the waveguide. We suppose that the injected REB is formed by a magnetically isolated diode.<sup>31</sup>

We have analyzed the evolution of the amplitude spectra of the current oscillations of a beam part reflected from the VC to the injection plane with the change of the beam current  $I_0$  and the value of external magnetic field induction  $B_0$ . Such current signals reflect VC space-time behavior and, hence, their analysis allows to reveal intrinsic electron beam dynamics and the characteristics of a possible relativistic vircator radiation for different system parameters. The spectrum corresponding to the subcritical regime of the system operation when beam current is less than the critical space-charge limited current  $I_{cr}(B_0)$  for the given external magnetic field is low-power and has a noise-type form. Note, the critical current is known to be the function of the magnetic field induction  $B_0$ .<sup>24,32,33</sup>

With the growth of beam current the relativistic vircator system goes into the supercritical regime, and the spectral component at the frequency of  $\omega_{VCO}$  ( $f_{VCO} \approx 21.7$  GHz for the case shown in Fig. 1(a)) with satellites appear in the spectrum of current oscillations, which are characterized by the significant chaotic dynamics (see frame in Fig. 1(a)). The position of this fundamental component is determined by the value of the plasma frequency,  $\omega_p^d$ , of the disturbed REB:  $\omega_{VCO} \approx \omega_p^d$ . The  $\omega_p^d$  value (disturbed plasma frequency) is proportional to the plasma frequency reduction factor<sup>31,34</sup> and the beam space charge density in the VC area that is defined by the electron focusing/defocusing processes during a beam propagation. Let us apply a factor  $k$  relating plasma frequencies of undisturbed and disturbed beams as  $\omega_p^d = k\omega_p^0$ . This factor takes into account both focusing/defocusing and plasma reduction effects and equals to 0.8 for the case shown in Fig. 1(a). Note that it is proportional to the degree of focusing of an electron beam in a VC area by means of the applied magnetic field.

The spectrum in Fig. 1(a) also demonstrates the presence of the higher harmonics  $n\omega_p^d$  of the disturbed plasma frequency up to  $n = 7$ . Besides, the quantity of the satellites of the  $n$ th harmonic increases with the number  $n$ . It corresponds to the complex relaxation-like oscillations of the VC in the system with the fundamental frequency being equal to the disturbed plasma frequency. Let us introduce

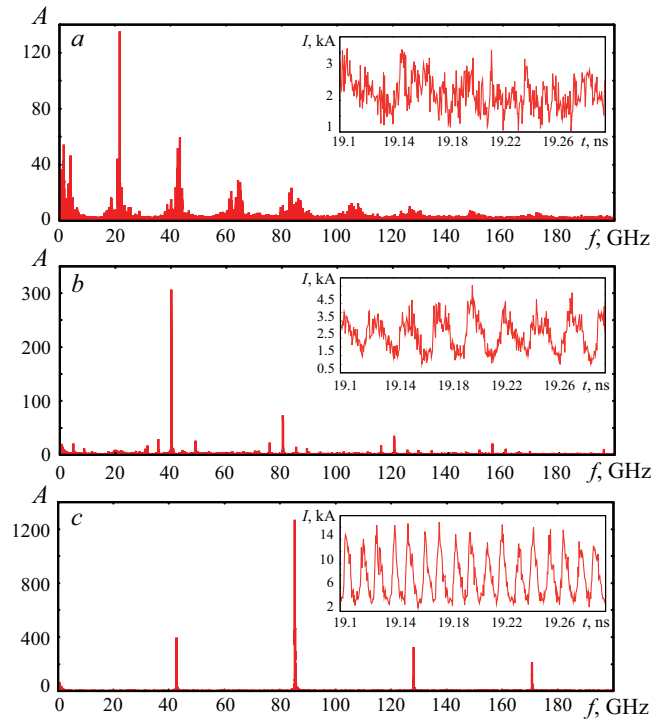


FIG. 1. The amplitude spectra of the current oscillations in the typical regimes: (a) supercritical regime when the VC oscillates at the  $\omega_{VCO} = \omega_p^d$  frequency and the fundamental harmonic ( $\sim 21.7$  GHz) of this frequency is maximal ( $I_0 = 16$  kA), (b) VCO's regime when the VC oscillates at the  $\omega_{VCO} = 2\omega_p^d$  and the fundamental harmonic ( $\sim 40.2$  GHz) of this frequency is maximal ( $I_0 = 18$  kA), (c) regime when  $\omega_{VCO} = 2\omega_p^d$  and the second harmonic ( $\sim 85.3$  GHz) of this frequency  $\omega_{VCO}$  is maximal ( $I_0 = 28$  kA). The short fragments of the time series of the analyzed current oscillations used for the spectra calculations are shown in the frames. Magnetic field is  $B_0 = 1.2$  T.

the normalized parameter of current supercriticality  $\delta I(B_0) = I_0/I_{cr}(B_0)$  determined by the ratio of the certain fixed REB current  $I_0$  to the beam critical (space-charge limited) current  $I_{cr}(B_0)$ .<sup>24,35</sup> The supercriticality parameter  $\delta I(B_0)$  characterizes the degree of development of VC oscillations in an electron beam and depends (for the fixed beam current  $I_0$ ) on a magnetic field induction value,  $B_0$ . We have found out that the observed VC dynamics at the  $\omega_p^d$  frequency is developed for the relatively small values of the supercriticality parameter: from  $\delta I(B_0) < 1.1$  for the weak magnetic fields  $B_0 < 0.1$  T to  $\delta I(B_0) < 2.5$  for  $B_0 > 0.5$  T.

With further increase of the current supercriticality parameter the consecutive qualitative change of the spectrum of the current oscillations occurs in the considered vircator system. First of all, switching of the fundamental spectral component from  $\omega_p^d$  to  $2\omega_p^d$  ( $f_{VCO} \approx 40.2$  GHz) takes place (Fig. 1(b)), with the current oscillations becoming more regular (see frame in Fig. 1(b)). The higher harmonics of the fundamental component and its modulation satellites are also present in the spectrum, with the amplitudes of all harmonics increasing in comparison with the case of smaller current supercriticality. The supercriticality parameter range, where such system dynamics is observed, varies for different external magnetic fields from [1.1, 2.6] for the weak magnetic fields  $B_0 < 0.1$  T to [2.5, 2.7]—for the stronger magnetic

fields  $B_0 > 0.5$  T. It indicates that the VC goes into a developed oscillatory regime when the parameter  $\delta I(B_0)$  overcomes a certain threshold value. Note that a factor  $k$  equals to 0.7 for the case shown in Fig. 1(b) that tells about the decrease of the degree of electron beam focusing in the VC area in comparison with the case of smaller current (for Fig. 1(a)). The plasma frequency reduction factor remains constant with the change of the beam current, the energy and the external magnetic field since it depends only on the system geometry.

The tendency of the growth of the amplitudes of higher harmonics (particularly, the second harmonic) in the spectrum of the current oscillations with the further increase of the current supercriticality parameter  $\delta I$  is found out in the analysis of the relativistic vircator model. Actually, Fig. 1(c) demonstrates the spectrum when the second harmonic of the fundamental component is maximal (the frequency of the fundamental component is  $\omega_{VCO} = 2\omega_p^d = 43$  GHz in this case). In this regime, the current oscillations waveform also changes sufficiently, the sharp peaks are well pronounced on time series (cf. frames in Figs. 1(b) and 1(c)). So, the investigated vircator is characterized by the regimes of the operation with the intense higher harmonics of the fundamental component. In turn, a factor  $k$  equals to 0.6 in this case, i.e., the degree of electron beam focusing in a VC area has become even less for the greater beam current value that is the consequence of the increased space charge forces.

Fig. 2 shows the dependency of the factor  $k$  on the beam current value  $I_0$  for the fixed external magnetic field  $B_0 = 1.2$  T. One can see that it demonstrates the monotonous decrease with the growth of  $I_0$  due to the rise of defocusing space charge forces.<sup>36</sup> Conventionally, this dependency may be divided into three specific ranges (I, II, and III in Fig. 2) with the qualitatively different spectra of the current oscillations which are characterized by different relations between the maximal spectral component and the disturbed plasma frequency,  $\omega_p^d$ . When the beam current value lies in the first range (I:  $10 < I_0 < 18$  kA,  $0.7 < k < 1$ ), the maximal component in the spectrum is the fundamental harmonic at the frequency  $\omega_p^d$  in the third region (III:  $I_0 > 20$  kA,  $k < 0.67$ ), the fundamental component corresponds to the frequency  $2\omega_p^d$ , and the second harmonic of it is maximal because of a

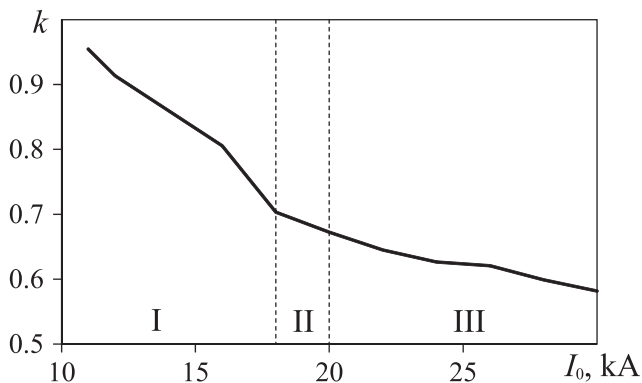


FIG. 2. The dependency of the factor  $k$  on a beam current  $I_0$  for the fixed external magnetic field  $B_0 = 1.2$  T. Roman numerals denote the areas with qualitatively different dynamics.

strong system nonlinearity. Finally, the second narrow area (II:  $18 < I_0 < 20$  kA,  $0.67 < k < 0.7$ ) is a transition region where the frequency of the fundamental harmonic becomes equal to  $2\omega_p^d$  and it is maximal in the spectrum.

The discovered switching of the fundamental spectral component from  $\omega_p^d$  to  $2\omega_p^d$  occurs when the dynamics of the REB with a VC is changed qualitatively. Actually, when the fundamental component has the frequency  $\omega_p^d$  (region I) the VC is characterized by a strongly nonuniform distribution at the azimuthal direction with one lumped space-charge potential minimum rotating at time (this minimum corresponds to the primary area of the VC reflected electrons). For the case when the frequency of the fundamental component is doubled (region II), the structure of the VC demonstrates the other character form with two rotating potential minima at the azimuthal direction. The appearance of the second minimum explains the effect of the fundamental frequency doubling. Physical mechanisms responsible for the discovered VC structure transformations are associated with the features of the azimuthal instability development and the excitation of the azimuthal rotational modes in a REB.<sup>10,24</sup>

We have also discovered that the described switching of the fundamental spectral component occurs when the beam radius overcomes a certain threshold value  $R_{th}$  which is different for various external magnetic fields. So, it means that the fundamental component switching occurs when the boundary electrons reaching this threshold radius are not restrained by the focusing magnetic field. It corresponds to the case when the sum of the defocusing forces (Coulomb force and centrifugal force) begins to exceed the focusing force of the magnetic field at radius  $R_{th}$ . So, for the fixed magnetic field,  $B_0$ , we can estimate analytically the typical beam current value when such change in the balance of the forces occurs.

Let us assume that the external magnetic field is strong enough to neglect the influence of the self-magnetic fields. Let the REB with the current  $I_0$  has the radius  $R_b$  at the injection plane and the radius  $R_{th} = bR_b$  in the VC area. The threshold  $R_{th}$  and corresponding  $b > 1$  depend on the external magnetic field and are determined by a numerical simulation. Moving in the system between the points with radii  $R_b$  and  $R_{th}$  in the presence of the constant external magnetic field electrons acquire an angular momentum. This momentum is proportional to the difference of induction fluxes across the cross-sections of the REB at the points with radii  $R_b$  and  $R_{th}$ , respectively:<sup>31</sup>

$$R_{th}^2 \frac{d\theta}{dt} = \frac{\eta B_0}{2\gamma_0} (R_{th}^2 - R_b^2), \quad (1)$$

where  $d\theta/dt$  is the azimuthal velocity of electrons. The motion of the electrons of the REB is determined by the action of the centrifugal force  $F_c = \gamma_0 m_e r (d\theta/dt)^2$ , Coulomb's repulsion force  $F_k = -eE_r$  and Lorentz force  $F_L = -er (d\theta/dt)B_0$  (here  $e$  and  $m_e$  are the charge and the mass of electron, respectively,  $r$  is the radial coordinate of electron,  $E_r$  is the radial component of the space charge field intensity). Then, one can write the motion equation for the boundary electron of the beam, taking into account the above, relation (1) and the equation  $d^2r/dt^2 = (2\eta V_0/\gamma_0)d^2r/dz^2$ :

$$\frac{d^2r}{dz^2} + \frac{\eta B_0^2}{8V_0\gamma_0} b R_b [1 - b^{-4}] - \frac{I_0 \sqrt{\gamma_0}}{4\pi\epsilon_0 \sqrt{2}\eta V_0^{3/2} b R_b} = 0, \quad (2)$$

where  $V_0$  is the accelerating voltage.

Equation (2) implies that for the fixed external magnetic field,  $B_0$ , there is typical beam current value  $I_{ch}$  for which REB keeps the constant radius,  $R_{th}$ , in the system. Actually, if we put  $d^2r/dz^2 = 0$  in Eq. (2) (it means the lack of the acceleration in the radial direction), we may easily obtain the value of this typical current  $I_{ch}$  for the fixed external magnetic field:

$$I_{ch} = \frac{\pi\epsilon_0 B_0^2 \eta^{3/2} \sqrt{V_0} R_b^2}{\sqrt{2}\gamma_0^{3/2}} (b^2 - b^{-2}). \quad (3)$$

When the beam current,  $I_0$ , exceeds  $I_{ch}$  the defocusing forces become greater than the focusing one and, as a consequence, the great part of electrons go beyond the threshold radius  $R_{th}$ . So,  $I_{ch}$  corresponds to the current when the switching of the fundamental spectral component from  $\omega_p^d$  to  $2\omega_p^d$  occurs. Actually, for the considered parameters ( $B_0 = 1.2$  T;  $b = 1.47$ ) Eq. (3) gives  $I_{ch} \approx 18.8$  kA which is in good agreement with the results of the numerical simulations. Indeed, the current value corresponding to the middle of the transition range II in Fig. 2, where the frequency of the fundamental spectral component switches from  $\omega_p^d$  to  $2\omega_p^d$ , approximately equals to 19 kA.

For the detailed analysis of the operating regimes of the relativistic vircator model with the control parameters variations, the regime map in the plane ( $I_0, B_0$ ) has been obtained (Fig. 3). Fig. 3 demonstrates three typical regimes: subcritical (region 1), supercritical with the maximal fundamental component in the spectrum of the current oscillations (2) and supercritical with the maximal second harmonic of the fundamental component (3). The basic tendency here is that with the beam current increase for different external magnetic fields we observe firstly the switching from the subcritical to supercritical regime and then the increase of the second harmonic of the fundamental component that leads finally to its domination in the spectrum (see region 3 in Fig. 3). At the same time, the amplitudes of the higher

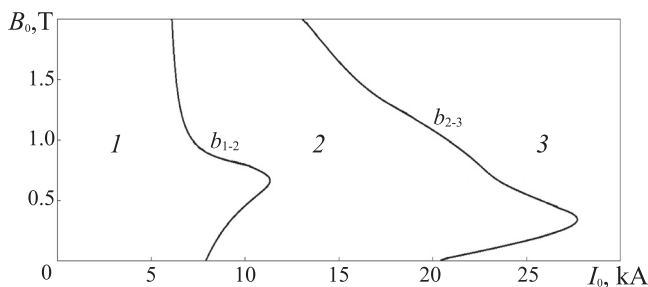


FIG. 3. The typical operating regimes of the vircator in the “beam current  $I_0$ —external magnetic field  $B_0$ ” plane. Region (1) corresponds to subcritical regime without VC formation (when beam current  $I_0 < I_{cr}(B_0)$ ), (2)—supercritical regime when the fundamental harmonic  $\omega_{VC0}$  in the spectrum of current oscillations is maximal, (3)—regime when the second harmonic of the fundamental component  $2\omega_{VC0}$  is maximal. Symbols  $b_{1-2}$  and  $b_{2-3}$  denote boundaries between regimes (1 → 2) and (2 → 3) correspondingly.

harmonics with numbers  $n > 2$  also increase with the growth of the beam current.

Note that the boundaries between the regimes,  $b_{1-2}$  and  $b_{2-3}$ , have the similar form in Fig. 3. The curve  $b_{1-2}$  is the dependency of the critical beam current,  $I_{cr}(B_0)$ , on the external magnetic field value. Its form and the presence of the area of the critical current growth are determined by the process of azimuthal instability development in a REB (the detailed discussions of this effect see in Ref. 24). The azimuthal instability development results in the decrease of space charge density at the VC area and, as a consequence, the increase of the critical beam current.

So, the analogous behavior of both boundaries indicates that the azimuthal instability also influences on the conditions of the switching from regime 2 to regime 3, and this switching occurs when space charge density at the VC area overcomes a certain character value. Indeed, when external magnetic field is relatively weak ( $B_0 < 0.4$  T) its growth leads to the decrease of the space charge density at the VC area due to the azimuthal instability development<sup>10,24</sup> and, therefore, the boundary curve  $b_{2-3}$  demonstrates the increase of the critical current in the range of  $B_0$  values. The stronger external magnetic fields ( $B_0 > 0.4$  T) suppresses the azimuthal instability<sup>10,24</sup> and focuses the electron beam resulting in space charge density growth. As a consequence, the specific beam current value decreases monotonously along the boundary  $b_{2-3}$  for  $B_0 > 0.4$  T.

Fig. 4 shows the dependencies of the amplitudes of the 1st—6th harmonics of the fundamental component in the spectrum of the current oscillations of the beam reflected from VC on the injected beam current  $I_0$ . The analysis allows to define the conditions (beam currents) when the higher harmonics are mostly developed in the spectrum and maximal energy is stored in these components. Actually, when  $I_0 \approx 24$  kA or  $I_0 \approx 28$  kA all six harmonics (except 6th harmonic for  $I_0 \approx 24$  kA) demonstrate the clearly defined local maxima for such external magnetic field, and the second harmonic strongly predominates over others for these values of the beam current. Note that practically for all values of the beam current corresponding to the development regime of

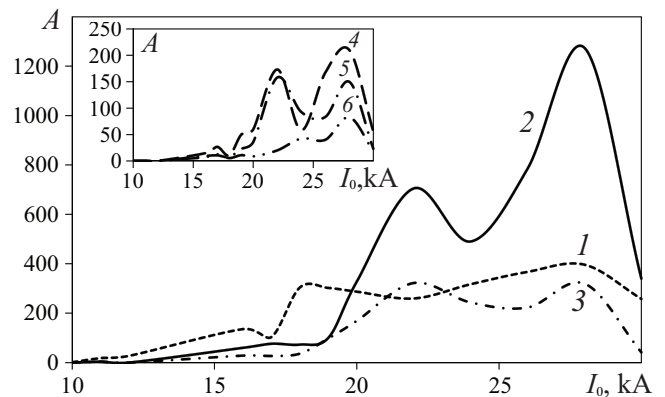


FIG. 4. The dependencies of the amplitudes of the first (curve 1), the second (2), the third (3), the fourth (curve 4 in the insert), the fifth (5 in the insert) and the sixth (6 in the inset) harmonics of the fundamental component in the spectrum of current oscillations on the beam current  $I_0$  for the fixed external magnetic field  $B_0 = 1.2$  T.

the vircator operation ( $I_0 > 20$  kA), the second harmonic has a maximal amplitude (the exception is the weakly overcritical regime ( $I_0 < 20$  kA) where the fundamental harmonic is maximal).

In conclusion, we have shown by means of 3D numerical simulation that the investigated vircator system demonstrates the tendency to the sufficient growth of the amplitudes of the higher harmonics in the spectrum of microwave oscillations with the increase of the beam current. The obtained results allow us to consider virtual cathode oscillators as promising high-power mmw-to-THz sources.

We thank Dr. S. V. Eremina for the English language support. This work has been supported by the Russian Science Foundation (Grant No. 14-12-00222).

- <sup>1</sup>D. J. Sullivan, J. E. Walsh, and E. A. Coutsias, *Virtual Cathode Oscillator (vircator) Theory*, High Power Microwave Sources (Artech House Microwave Library, NY, 1987), Vol. 13.
- <sup>2</sup>S. H. Gold and G. S. Nusinovich, *Rev. Sci. Instrum.* **68**, 3945 (1997).
- <sup>3</sup>J. Benford, J. A. Swegle, and E. Schamiloglu, *High Power Microwaves* (CRC Press, Taylor and Francis, 2007).
- <sup>4</sup>R. A. Mahaffey, P. A. Sprangle, J. Golden, and C. A. Kapetanacos, *Phys. Rev. Lett.* **39**, 843 (1977).
- <sup>5</sup>A. E. Hramov, A. A. Koronovskii, and S. A. Kurkin, *Phys. Lett. A* **374**, 3057 (2010).
- <sup>6</sup>A. E. Dubinov and V. D. Selemir, *J. Commun. Technol. Electron.* **47**, 575 (2002).
- <sup>7</sup>A. E. Dubinov, Yu. I. Kornilova, and V. D. Selemir, *Phys.-Usp.* **45**, 1109 (2002).
- <sup>8</sup>D. Biswas, *Phys. Plasmas* **16**, 063104 (2009).
- <sup>9</sup>R. A. Filatov, A. E. Hramov, Y. P. Bliokh, A. A. Koronovskii, and J. Felsteiner, *Phys. Plasmas* **16**, 033106 (2009).
- <sup>10</sup>S. A. Kurkin, A. E. Hramov, and A. A. Koronovskii, *Appl. Phys. Lett.* **103**, 043507 (2013).
- <sup>11</sup>S. C. Burkhart, R. D. Scarpetty, and R. L. Lundberg, *J. Appl. Phys.* **58**, 28 (1985).
- <sup>12</sup>R. F. Hoeberling and M. V. Fazio, *IEEE Trans. Electromagn. Compatib.* **34**, 252–258 (1992).
- <sup>13</sup>A. E. Hramov, A. A. Koronovskii, S. A. Kurkin, and I. S. Rempen, *Int. J. Electron.* **98**, 1549 (2011).
- <sup>14</sup>K. R. Clements, R. D. Curry, R. Druce, W. Carter, M. Kovac, J. Benford, and K. McDonald, *IEEE Trans. Dielectr. Electr. Insul.* **20**, 1085 (2013).
- <sup>15</sup>A. E. Dubinov, I. A. Efimova, K. E. Mikheev, V. D. Selemir, and V. P. Tarakanov, *Plasma Phys. Rep.* **30**, 496 (2004).
- <sup>16</sup>G. Singh and C. Shashank, *Phys. Plasmas* **18**, 063104 (2011).
- <sup>17</sup>R. Verma, R. Shukla, S. K. Sharma, P. Banerjee, R. Das, P. Deb, T. Prabaharan, B. Das, E. Mishra, B. Adhikary, K. Sagar, M. Meena, and A. Shyam, *IEEE Trans. Electron Devices* **61**, 141 (2014).
- <sup>18</sup>J. H. Booske, *Phys. Plasmas* **15**, 055502 (2008).
- <sup>19</sup>P. H. Siegel, *IEEE Trans. Microwave Theory Tech.* **50**, 910 (2002).
- <sup>20</sup>K. Kawase, Y. Ogawa, Y. Watanabe, and H. Inoue, *Opt. Express* **11**, 2549 (2003).
- <sup>21</sup>B. Ferguson and X. C. Zhang, *Nature Mater.* **1**, 26 (2002).
- <sup>22</sup>C. M. Mann, *Terahertz Sources and Systems* (Kluwer, Dordrecht, 2001).
- <sup>23</sup>Z. Yang, G. Liu, H. Shao, J. Sun, Y. Zhang, H. Ye, and M. Yang, *IEEE Trans. Plasma Sci.* **41**, 3604 (2013).
- <sup>24</sup>A. E. Hramov, S. A. Kurkin, A. A. Koronovskii, and A. E. Filatova, *Phys. Plasmas* **19**, 112101 (2012).
- <sup>25</sup>T. Saito, N. Yamada, and S. Ikeuti, *Phys. Plasmas* **19**, 063106 (2012).
- <sup>26</sup>M. K. Hornstein, V. S. Bajaj, R. G. Griffin, K. E. Kreischer, I. Mastovsky, M. A. Shapiro, J. R. Sirigiri, and R. J. Temkin, *IEEE Trans. Electron Devices* **52**, 798 (2005).
- <sup>27</sup>V. L. Bratman, A. E. Fedotov, Y. K. Kalynov, V. N. Manuilov, M. M. Ofitserov, S. V. Samsonov, and A. V. Savilov, *IEEE Trans. Plasma Sci.* **27**, 456 (1999).
- <sup>28</sup>T. Notake, T. Saito, Y. Tatematsu, A. Fujii, S. Osagawara, L. Agusu, I. Ogawa, T. Idehara, and V. N. Manuilov, *Phys. Rev. Lett.* **103**, 225002 (2009).
- <sup>29</sup>D. V. Vyalykh, A. E. Dubinov, V. S. Zhdanov, I. L. L'vov, S. A. Sadovoi, and V. D. Selemir, *Tech. Phys. Lett.* **39**, 217 (2013).
- <sup>30</sup>H. E. Brandt, *IEEE Trans. Plasma Sci.* **13**, 513 (1985).
- <sup>31</sup>S. E. Tsimring, *Electron Beams and Microwave Vacuum Electronics* (John Wiley and Sons, Inc., Hoboken, New Jersey, 2007).
- <sup>32</sup>A. E. Hramov, A. A. Koronovskii, M. Yu. Morozov, and A. V. Mushtakov, *Phys. Lett. A* **372**, 876 (2008).
- <sup>33</sup>S. A. Kurkin and A. E. Hramov, *Tech. Phys. Lett.* **35**, 23 (2009).
- <sup>34</sup>J. D. Lawson, *The Physics of Charged-particle Beams*, Monographs on Physics (Oxford University Press, 1977).
- <sup>35</sup>V. L. Granatstein and I. Alexeeff, *High Power Microwave Sources* (Artech House Microwave Library, 1987).
- <sup>36</sup>S. A. Kurkin, A. A. Koronovskii, and A. E. Hramov, *Tech. Phys. Lett.* **37**, 356 (2011).